Cellular/Molecular

Synaptic Release Generates a Tonic $GABA_A$ Receptor-Mediated Conductance That Modulates Burst Precision in Thalamic Relay Neurons

Damian P. Bright,[1] M. Isabel Aller,[2] and Stephen G. Brickley[1]

[1]Biophysics Section, Blackett Laboratory, Imperial College, London SW7 2AZ, United Kingdom, and [2]Instituto de Neurociencias de Alicante, Consejo Superior de Investigaciones Científicas–Universidad Miguel Hernandez, 03550 Sant Joan d'Alacant, Spain

Tonic inhibition has emerged as a key regulator of neuronal excitability in the CNS. Thalamic relay neurons of the dorsal lateral geniculate nucleus (dLGN) exhibit a tonic $GABA_A$ receptor ($GABA_AR$)-mediated conductance that is correlated with δ-subunit expression. Indeed, consistent with the absence of δ-subunit expression, no tonic conductance is found in the adjacent ventral LGN. We show that, in contrast to the situation in cerebellar granule cells, thalamic δ-subunit-containing $GABA_A$Rs (δ-$GABA_A$Rs) do not contribute to a spillover component of IPSCs in dLGN. However, tonic activation of thalamic δ-$GABA_A$Rs is sensitive to the global level of inhibition, showing an absolute requirement on the synaptic release of GABA. Thus, the tonic conductance is abolished when transmitter release probability is reduced or action potential-evoked release is blocked. We further show that continuous activation of δ-$GABA_A$Rs introduces variability into the timing of low-threshold rebound bursts. Hence, activation of δ-$GABA_A$Rs could act to destabilize thalamocortical oscillations and therefore have an important impact on behavioral state.

Key words: **$GABA_A$ receptor; δ-subunit; tonic inhibition; synaptic release; thalamic relay neuron; burst firing**

Introduction

The control of network activity by GABAergic mechanisms can involve the activation of multiple $GABA_A$ receptor ($GABA_AR$) types. In the thalamus, $GABA_A$ receptors formed from $\alpha\beta\gamma$ subunit assemblies are targeted to synapses and give rise to temporally discrete phasic inhibition (Soltesz et al., 1990; Okada et al., 2000; Pirker et al., 2000; Sassoe-Pognetto et al., 2000; Peng et al., 2002). In addition, a large population of extrasynaptic $GABA_A$ receptors was first described in thalamic relay neurons (Soltesz et al., 1990) and have now been attributed to the expression of δ-subunit-containing $GABA_A$Rs (δ-$GABA_A$Rs) (Sur et al., 1999; Jia et al., 2005; Kralic et al., 2006). Because these δ-$GABA_A$ receptors exhibit an unusually high affinity for GABA (Saxena and Macdonald, 1996; Brown et al., 2002), they are ideally suited to the generation of the tonic $GABA_A$ receptor-mediated conductance that is found in relay neurons of the ventrobasal thalamus (Porcello et al., 2003; Belelli et al., 2005) and dorsal lateral geniculate nucleus (dLGN) (Cope et al., 2005). However, extrasynaptic δ-$GABA_A$Rs are unlikely to be present in all thalamic nuclei. For example, the δ subunit is expressed heavily in the anteroventral nucleus but is virtually absent from the adjacent laterodorsal thalamic nucleus (Kralic et al., 2006). A similar pattern is observed across the LGN with α4 and δ subunits expressed heavily in the dLGN compared with virtually no subunit expression in the ventral LGN (vLGN) (Pirker et al., 2000; Peng et al., 2002; Kralic et al., 2006). These differential expression patterns make thalamic areas such as the LGN attractive for examining the functional significance of δ-$GABA_A$Rs.

The shunting inhibition produced by activation of δ-$GABA_A$Rs has been shown to alter the integrative properties of a neuron (Brickley et al., 2001; Hamann et al., 2002; Mitchell and Silver, 2003; Stell et al., 2003; Farrant and Nusser, 2005) and may also influence the character of any network oscillation (Cope et al., 2005; Maguire et al., 2005; Vida et al., 2006). Specifically, there is evidence that the tonic conductance can regulate thalamocortical oscillations by contributing to a characteristic switch in thalamic relay neuron excitability (Cope et al., 2005). Although tonic $GABA_AR$-mediated conductances have now been identified in many neuronal populations (for review, see Farrant and Nusser, 2005), the source of the GABA responsible for continuously activating extrasynaptic δ-$GABA_A$Rs is not clear. For example, in mature cerebellar granule cells, spontaneous $GABA_A$ receptor-mediated synaptic currents are rare, and the tonic $GABA_A$ receptor-mediated conductance is not produced by conventional vesicular release of GABA from interneurons (Wall and Usowicz, 1997; Rossi et al., 2003). These observations leave open the question of how tonic inhibition could participate in the dynamic control of neuronal excitability if its magnitude is not regulated by conventional release mechanisms (De Schutter, 2002; Farrant and Nusser, 2005). We have developed an acute slice preparation from adult mice that contains a clearly delineated dLGN and

Received Nov. 24, 2006; revised Jan. 10, 2007; accepted Feb. 1, 2007.

This work was supported by a Wellcome Trust project grant (S.G.B.). We thank Mark Farrant for helpful comments on a previous version of this manuscript.

Correspondence should be addressed to Dr. Stephen G. Brickley, Biophysics Section, Blackett Laboratory, Imperial College, South Kensington, London SW7 2AZ, UK. E-mail: s.brickley@imperial.ac.uk.

DOI:10.1523/JNEUROSCI.5100-06.2007

 0270-6474/07/272560-10$15.00/0

vLGN to explore further the functional significance of extrasynaptic δ-$GABA_A$Rs.

Materials and Methods

Slice preparation. All experiments were performed on brain slices obtained from mature (at least 1 month postnatal) male C57BL/6 mice, in accordance with the Animals (Scientific Procedures) Act of 1986. In brief, the brain was rapidly removed and placed in ice-cold slicing solution composed of the following (in mM): 85 NaCl, 2.5 KCl, 1 $CaCl_2$, 4 MgCl, 1.25 NaH_2PO_4, 26 $NaHCO_3$, 75 sucrose, 25 glucose, pH 7.4 when bubbled with 95% O_2 and 5% CO_2. Coronal slices (250 μm thick) were cut at the level of the hippocampus using a moving blade microtome (DSK Super Zero 1; Dosaka EM, Kyoto, Japan). The slices were then incubated at 37°C for 30 min, after which the high-sucrose slicing solution was gradually replaced with normal recording solution over a period of ~30 min. Slices were then maintained at room temperature in this solution, bubbled with 95% O_2/5% CO_2, until required.

Recording procedures and analysis. Slices were continuously perfused at physiological temperatures (35–38°C) with recording solution containing the following (in mM): 125 NaCl, 2.5 KCl, 2 $CaCl_2$, 1 MgCl, 1.25 NaH_2PO_4, 26 $NaHCO_3$, 25 glucose, pH 7.4 when bubbled with 95% O_2 and 5% CO_2. Thalamic neurons in the LGN were visually identified using a Zeiss (Jena, Germany) Axioskop FS microscope equipped with differential interference contrast-infrared optics. Whole-cell and cell-attached recordings were made under voltage clamp using a Multiclamp 700B amplifier (Molecular Devices, Union City, CA). Recording electrodes were pulled from thick-walled borosilicate glass (GC-150F-10; Harvard Apparatus, Edenbridge, UK) and had a resistance of 5–8 MΩ when filled with intracellular solution containing the following (in mM): 140 CsCl, 4 NaCl, 0.5 $CaCl_2$, 10 HEPES, 5 EGTA, 2 Mg-ATP; the pH was adjusted to 7.3 with CsOH. The fluorescent dyes Lucifer yellow or Alexa 488 were included in the electrode solution (0.5 mg/ml; Sigma, Poole, UK) to allow for later confocal imaging of filled neurons. During whole-cell recording, $GABA_A$ receptor-mediated conductances were pharmacologically isolated by inclusion of the ionotropic glutamate receptor blocker kynurenic acid (0.5 mM) in the recording solution. The following drugs were added to the recording solution as required: 4,5,6,7-tetrahydroisothiazolo-[5,4-c]pyridin-3-ol (THIP), tetrodotoxin (TTX), and 2-(3-carboxypropyl)-3-amino-6-(4-methoxyphenyl)-pyridazinium bromide (SR-95531) (all from Sigma). The fast blocking action of SR-95531 at a high 20 μM concentration probably reflects the high affinity of the $GABA_A$ receptors, coupled with the fact that we use fast flow rates of 4–5 ml/min to keep the adult slices healthy for reasonable periods of time. Moreover, this observation is consistent with other studies that used saturating concentrations of a high-affinity antagonist (Rossi et al., 2003; Stell et al., 2003; Cope et al., 2005). For experiments looking at the Ca^{2+} dependence of currents, the concentration of MgCl was adjusted to compensate for the reduction in $CaCl_2$. For cell-attached recording, electrodes were filled with extracellular recording solution and no antagonists were present in the bath solution. A few whole-cell current-clamp recordings were also performed using an intracellular solution containing (in mM): 120 KCH_3SO_4, 4 NaCl, 1 $MgCl_2$, 1 $CaCl_2$, 10 HEPES, 10 EGTA, 3 Mg-ATP, 0.3 Na-GTP; the pH was adjusted to 7.3 with KOH.

Online data acquisition and off-line analysis were performed using the Strathclyde Electrophysiology software WinEDR/WinWCP (John Dempster, University of Strathclyde, Glasgow, UK). Current records were low-pass filtered at 10 kHz and acquired at 20 kHz using a National Instruments (Austin, TX) board (NI-DAQmx, PCI-6221). For each cell, the series resistance, R_S, and input resistance, R_{in}, were calculated using the peak and steady-state current responses, respectively, to 10 mV hyperpolarizing voltage steps. We also calculated the seal resistance, R_{seal}, for each cell using the steady-state current response to hyperpolarizing steps applied in the cell-attached configuration. Recordings were only subjected to additional analysis if R_{seal} was >1 GΩ. The membrane capacitance was determined using a weighted time constant for the decay of the capacitive current transient, calculated as the integral of the transient divided by the peak current. From Gaussian fits to the input resistance distribution (data not shown), cells with an input resistance >500 MΩ were classified as interneurons. Unfortunately, in contrast to the relay neuron population, it has proven difficult to recover these small, high-resistance cells for subsequent morphological analysis. Spontaneous IPSCs (sIPSCs) were detected with amplitude- and kinetics-based criteria (events were accepted when they exceeded a threshold of 4–6 pA for 0.5 ms). Averaged IPSC waveforms were generally constructed using events detected over 30 s epochs (at least 50 uncontaminated IPSCs), and in the case of drug applications, these waveforms were calculated at least 60 s after the application. The weighted decay constant, $\tau_{integral}$, was calculated as the integral of the IPSC divided by the peak current. To compare the variability of populations of IPSCs, we used the coefficient of variation (CV), defined as the SD in a parameter divided by the mean value. At least 50 uncontaminated IPSCs were used to calculate CV values for each cell. The tonic $GABA_A$ receptor-mediated current was defined as the current blocked by SR-95531. To account for cell-to-cell variability, the tonic current was expressed as a conductance normalized to membrane capacitance (in picosiemens per picofarad). In the loose cell-attached configuration, we injected suprathreshold extracellular current steps to elicit a stable rebound burst. The amount of current required was found to vary between cells, dependent on the seal resistance. No steady-state current was applied.

Morphological analysis. After electrophysiological recording, slices were fixed in PBS containing 4% paraformaldehyde for 24 h. Slices were then washed in PBS, before being mounted in Vectashield mounting medium (Vector Laboratories, Burlingame, CA). Optical sections were obtained using a Zeiss LSM 510 upright confocal microscope, equipped with a 40× oil-immersion objective lens. Fluorescence was visualized using the 458 nm line of an argon laser, with emitted light passing through a 475 nm long-pass filter. Neurons were z-sectioned into 1 μm optical slices. The signal-to-noise ratio was improved by averaging at least two scans for each z-section.

In situ *hybridization. In situ* hybridization studies using ^{35}S-labeled oligonucleotide probes were performed according to the method described previously (Wisden and Morris, 2002). Three wild-type mouse brains were used for each probe. The oligonucleotide sequences used were as follows: δ, AGCAGCTGAGAGGGAGAAAAGGACGATGGCGTTCCT; α4, TTCTGGACAGAAACCATCTTCGCCACATGCCATACT.

To check for nonspecific labeling of brain sections, each radiolabeled oligonucleotide was hybridized with 100-fold excess of unlabeled oligonucleotide. Images were processed after a 4 week exposure using Biomax MR (Kodak, Rochester, NY) x-ray films.

Statistical analysis. Statistical tests were performed using STATISTICA 5.1 (StatSoft, Tulsa, OK) and considered significant at $p < 0.05$. A Shapiro–Wilk test was used to determine whether measures were normally distributed, and differences between groups were examined using the Student's *t* test. When distributions were not normal, the Mann–Whitney *U* test, Wilcoxon matched-pair test, or the Kolmogorov–Smirnov test were used, as indicated.

Results

A tonic $GABA_A$R-mediated conductance is only present in dLGN relay neurons

As shown in Figure 1*A*, α4 and δ $GABA_A$R subunits are expressed at high levels in the dLGN but are absent from the vLGN. This result is in clear agreement with antibody labeling studies performed in the rat (Pirker et al., 2000) and is consistent with the results obtained from other mouse strains used in recent anatomical studies (Peng et al., 2002; Kralic et al., 2006). Our recordings were made from mature thalamic neurons (66 ± 3 d, $n = 100$ mice) at 37.1 ± 0.04°C ($n = 141$ cells). From their location in the slice preparation, a total of 76 dLGN and 62 vLGN neurons were unambiguously identified (Fig. 1*B*). Neurons within dLGN were usually silent with spontaneous action potentials only evident in 19% (15 of 76) of recordings. This is similar to the situation reported by Cope et al. (2005). However, in vLGN the majority of cells (72%, 45 of 62) fired spontaneous action potentials at a

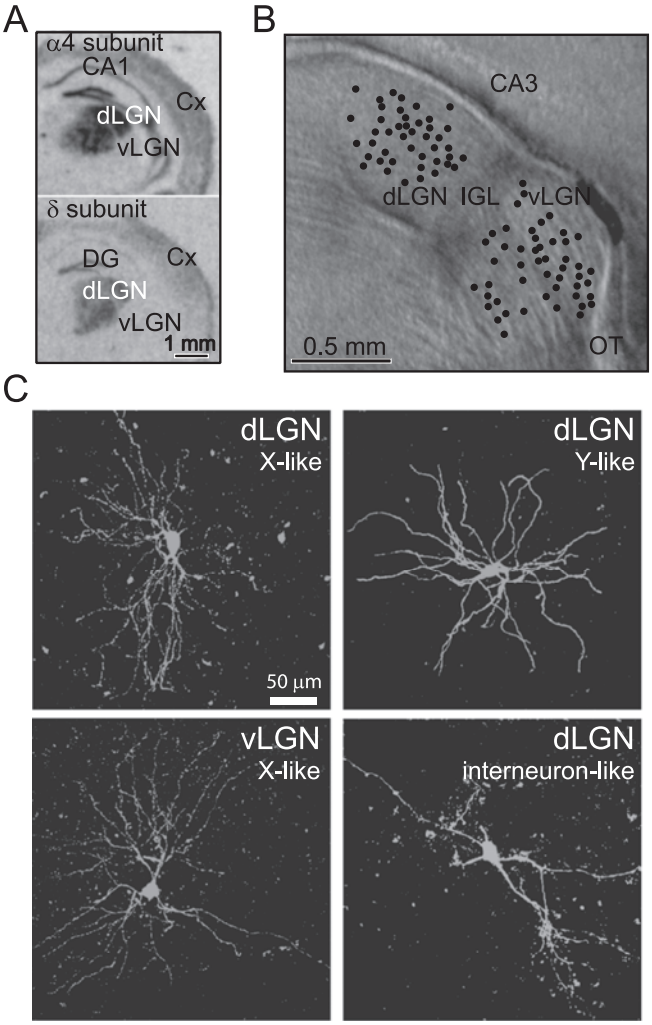

Figure 1. Morphological features of neurons recorded in dLGN and vLGN. ***A***, *In situ* hybridization data collected from coronal sections of adult C57BL/6 mice comparing the distribution of α4 and δ subunits in the hippocampal CA regions, dentate gyrus (DG), neocortex (Cx), dLGN, and vLGN. ***B***, The relative recording locations of all cells used in this study are shown superimposed on a single representative image of a thalamic slice preparation. IGL, Intergeniculate leaflet; OT, optic tract. ***C***, After electrophysiological recordings, it was possible to recover a number of cells for confocal imaging. The results of this imaging are shown for representative neurons in dLGN and vLGN.

frequency of 7.3 ± 1.1 Hz. This could indicate that vLGN relay neurons are resting more depolarized than dLGN relay neurons and therefore, are more likely to exhibit tonic firing. A fraction of these cells were recovered for subsequent morphological analysis ($n = 17$). As shown in Figure 1*C*, in dLGN, putative relay neurons were observed with both X- and Y-like properties. X-like neurons had a polar distribution of primary dendrites with obvious spines, compared with the radial distribution of smooth dendrites reported for Y-like neurons (Sherman and Guillery, 1996; Lam et al., 2005). No obvious Y-like morphology has thus far been encountered in the vLGN, and interneuron-like morphology was only observed for one recovered cell in both the dLGN and vLGN data sets. Analysis of input capacitance revealed the presence of two distinct cell populations (data not shown), with the larger cell population being more prevalent in the dLGN. The data set not only contains a large number of small cells, but also a proportion of these small cells display a high input resistance, indicative of local interneurons (Lere-sche et al., 1991; Pape et al., 1994; Williams et al., 1996; Zhu and Uhlrich, 1997; Zhu et al., 1999). Therefore, based on this measure, our data set has been divided into dLGN and vLGN relay neurons, and putative interneurons (see Materials and Methods).

In dLGN relay neurons, application of 20 μM SR-95531 caused a robust reduction in both the holding current (from −385.8 ± 66.0 pA to −273.4 ± 59.6 pA; $n = 37$) and the RMS baseline noise (from 3.6 ± 0.3 to 2.9 ± 0.3 pA). This reduction in holding current corresponds to a $GABA_A$R-mediated conductance of 54.2 ± 13.9 pS/pF. As illustrated in Figure 2*C*, application of SR-95531 did not significantly alter the holding current in recordings from vLGN relay neurons. The tonic $GABA_A$R-mediated conductance calculated in these cells was on average only 6.6 ± 4.1 pS/pF ($n = 14$). A lack of tonic $GABA_A$R-mediated conductance was also observed for thalamic interneurons (Fig. 2*B*), regardless of their location in dLGN or vLGN. Putative dLGN interneurons had a calculated tonic conductance of only 6.7 ± 4.5 pS/pF ($n = 6$), and vLGN interneurons also had an insignificant tonic conductance of 2.5 ± 0.9 pS/pF ($n = 20$).

In contrast to its action on the tonic conductance, 20 μM SR-95531 caused a complete block of spontaneous $GABA_A$R-mediated IPSCs in all dLGN and vLGN neuronal populations (Fig. 2*A*,*C*). Moreover, the average spontaneous IPSC frequency recorded from vLGN relay neurons was 6.1 ± 1.6 Hz, ($n = 17$) compared with 7.9 ± 2.1 Hz ($n = 39$) in dLGN relay neurons, demonstrating that there was no significant difference in the frequency of GABA release in these two nuclei. Therefore, the absence of a tonic $GABA_A$R-mediated conductance in vLGN cannot be explained by reduced GABA release in this structure. The same is true of the putative interneuron population within the vLGN, which displays a similar frequency of spontaneous GABA release (5.9 ± 1.6 Hz; $n = 22$) but once again exhibit no significant $GABA_A$R-mediated tonic conductance (Fig. 2*D*). Analysis of putative interneurons within the dLGN also demonstrated that a high sIPSC frequency (7.9 ± 3.5 Hz, $n = 10$) can occur in the absence of a tonic $GABA_A$R-mediated conductance. Therefore, the presence of a tonic $GABA_A$R-mediated conductance correlates well with the expression of δ-$GABA_A$Rs in adult dLGN, but this tonic conductance appears to be restricted to thalamic relay neurons.

As shown in Table 1, despite the presence of a tonic $GABA_A$R conductance in dLGN, the sIPSCs still had a rapid monotonic rise, with an average 10–90% rise time of ~500 μs. As well as having comparable rise times, the range of decay times observed in dLGN and vLGN relay neurons were similar, and after constructing average waveforms, it was clear that sIPSC decay kinetics were no different in dLGN and vLGN relay neurons (for representative examples, see Fig. 3*B*,*E*; for population averages, see Table 1). Therefore, it could be argued that a spillover-like phenomenon involving activation of high-affinity δ-$GABA_A$Rs is not contributing to a slower IPSC decay in dLGN relay neuron. This is in contrast to the situation reported for cerebellar granule neurons, in which activation of receptors containing the α6 and δ subunits can generate a slow rising and decaying synaptic conductance that in turn leads to a slower IPSC decay (Rossi and Hamann, 1998; Hamann et al., 2002). The average IPSC peak amplitude was significantly larger in the vLGN population (see Table 1). It is clear from the representative examples shown in Figure 3, *B* and *E*, that this greater average peak amplitude is simply attributable to an increased contribution from larger sIPSCs with identical decay kinetics in the vLGN population. To

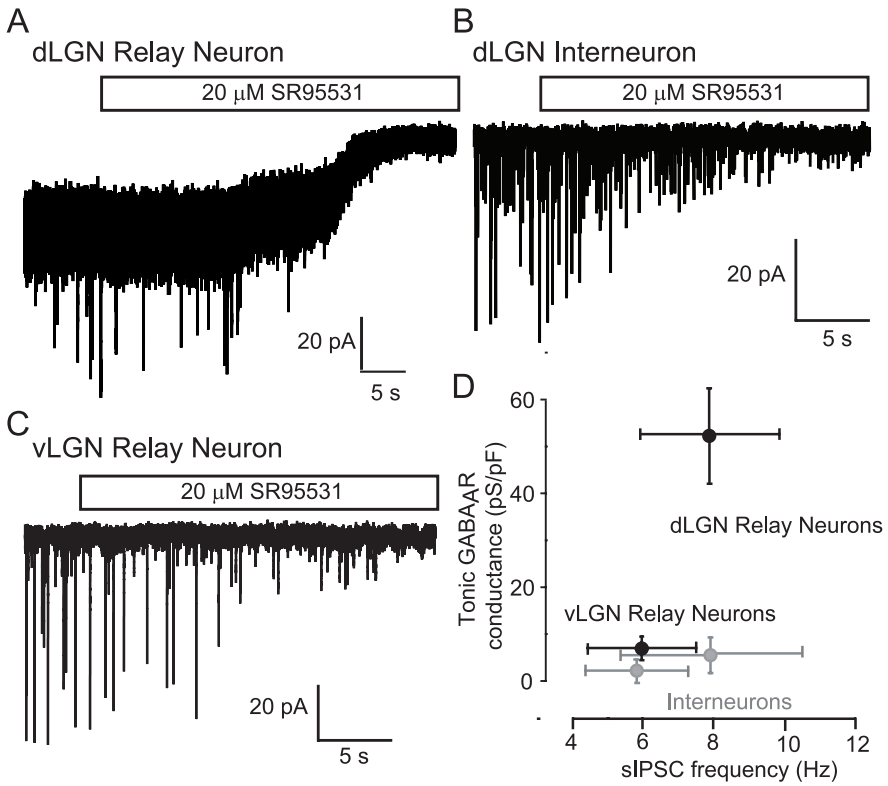

Figure 2. A tonic $GABA_A$R-mediated conductance is only present in dLGN relay neurons and is absent from vLGN relay neurons and all interneuron populations. ***A–C***, Representative current traces recorded at a holding potential of −60 mV from a dLGN relay neuron (***A***), a dLGN interneuron (***B***), and a vLGN relay neuron (***C***). In each trace, the transient inward deflections are sIPSCs that were completely abolished by the application of the $GABA_A$R antagonist SR-95531 (open bar). In contrast, a tonic $GABA_A$R-mediated conductance was only present in the dLGN relay neuron. In this cell, application of SR-95531 resulted in the block of a steady-state inward current and a reduction in the background noise associated with the current recording. ***D***, Quantification of the tonic $GABA_A$R-mediated conductance and the sIPSC frequency in all cells examined. Note that the tonic conductance is only present in the dLGN relay neuron population, but a similar sIPSC frequency is present in all neuronal populations.

further examine this point, we constructed all-point and cumulative histogram plots for all sIPSC peak amplitudes recorded from dLGN and vLGN relay neurons. As illustrated in Figure 3, *C* and *F*, there was no significance difference between the amplitude distributions recorded from the dLGN and vLGN (Kolmogorov–Smirnov test). Therefore, the increased noise associated with dLGN relay neurons does not appear to be masking small events.

The GABA giving rise to the tonic conductance arises from vesicular release

One central issue that has not been resolved in any adult brain region is the source of the GABA giving rise to the tonic conductance. Bath application of 500 nM TTX significantly reduced the IPSC frequency in dLGN relay neurons from 5.6 ± 3.0 to 1.8 ± 0.9 Hz ($n = 9$), indicating a reduction in the rate of vesicular GABA release (for a representative recording, see Fig. 4*A*,*B*; the inset of *B* quantifies the effect on the IPSC frequency in all cells). Although the frequency of IPSCs was significantly reduced in the presence of TTX, we did not observe any change in the peak amplitude or kinetics of the synaptic conductance. For the example shown in Figure 4, the range of peak amplitudes and decay times was very similar for both sIPSCs and mIPSCs, and this similarity is also reflected in the average waveforms (Fig. 4*C*,*D*, Table 1). The simplest explanation for the lack of a change in peak amplitude is that the synapses releasing GABA onto the dLGN relay neurons have a low release probability and therefore, during action potential-evoked release, there is little superposition of synaptic events. Furthermore, the fact that sIPSC and mIPSC kinetics were so similar would again suggest that spillover does not significantly influence IPSC kinetics. At the same time, during the course of this experiment, we did observe a clear reduction in the holding current in response to the decreased frequency of GABA release (Fig. 4*B*). To quantify this apparent change in the tonic conductance, we applied 20 μM SR-95531 at the end of the experiment. On average, the magnitude of the SR-95531-sensitive conductance was significantly reduced from 42.6 ± 17.9 to 5.6 ± 2.3 pS/pF ($n = 9$) in the presence of TTX. Therefore, blockade of action potential-dependent vesicular release leads to a complete loss of tonic $GABA_A$R-mediated conductance in the dLGN.

To further test the vesicular dependence of the tonic $GABA_A$R-mediated conductance, we altered the extracellular Ca^{2+} concentration ($[Ca^{2+}]_{ext}$). Figure 5 illustrates an experiment in which $[Ca^{2+}]_{ext}$ was raised from 1 to 2 mM. Altering release probability by changing $[Ca^{2+}]_{ext}$ did not affect the peak amplitude or kinetics of the IPSCs (Table 1). However, in parallel with an increase in the frequency of vesicular GABA release, this perturbation did result in a clear increase in the magnitude of the holding current. It is also clear from this particular cell that the holding current recorded in 1 mM $[Ca^{2+}]_{ext}$ was similar to that observed when all $GABA_A$Rs were blocked in the presence of 20 μM SR-95531. Indeed, in adult dLGN relay neurons, there was no significant tonic $GABA_A$R-mediated conductance (3.6 ± 1.2 pS/pF; $n = 7$) recorded in 1 mM $[Ca^{2+}]_{ext}$ (Fig. 5*C*). Furthermore, the rate of vesicular GABA release correlates well with the magnitude of this tonic conductance, because the average frequency of IPSCs was 4.4 ± 2.1 Hz ($n = 10$) in 1 mM $[Ca^{2+}]_{ext}$ compared with 7.1 ± 2.1 Hz in 2 mM $[Ca^{2+}]_{ext}$. Ca^{2+} shift experiments in vLGN relay neurons and interneurons of both dLGN and vLGN demonstrate that a tonic $GABA_A$R-mediated conductance is only found in dLGN relay neurons in the presence of 2 mM $[Ca^{2+}]_{ext}$ (Fig. 5*D*,*E*). Together, the TTX and Ca^{2+} shift data suggest that a sufficiently high rate of vesicular GABA release is necessary to raise the ambient GABA concentration such that extrasynaptic δ-$GABA_A$Rs will be persistently activated in dLGN relay neurons.

Low-threshold bursts can be elicited under conditions of unaltered internal Cl^- homeostasis

A recent study has demonstrated that the presence of a tonic $GABA_A$R-mediated conductance can favor burst firing in the dLGN because of the generation of a more hyperpolarized membrane potential (Cope et al., 2005). It is also clear that once a relay neuron is in burst mode, the input conductance will influence the timing and precision of low-threshold bursts (Zhan et al., 1999; Sohal et al., 2006). However, the input conductance of a neuron is likely to be altered in the whole-cell configuration because of the

Table 1. Properties of IPSCs recorded in dLGN and vLGN relay neurons and interneurons

Cell type	Recording conditions	Frequency (Hz)	Rise time (μs)	Peak amplitude (pA)	Decay time (ms)	*n*
dLGN relay neurons	2 mM $[Ca^{2+}]_{ext}$	7.3 ± 2.2	490.5 ± 28.4	−23.8 ± 3.4	6.4 ± 0.4	36
	1 mM $[Ca^{2+}]_{ext}$	4.4 ± 2.1	492.8 ± 39.8	−23.6 ± 5.3	6.2 ± 0.6	10
	500 nM TTX	1.8 ± 0.9*	553.6 ± 104.5	−16.9 ± 2.7	8.1 ± 1.6	9
	1 μM THIP	12.4 ± 6.4	512.5 ± 116.1	−18.7 ± 4.9	5.2 ± 1.0	4
Interneurons	2 mM $[Ca^{2+}]_{ext}$	7.9 ± 3.5	690.7 ± 66.3	−25.7 ± 3.5	9.7 ± 1.2	10
vLGN relay neurons	2 mM $[Ca^{2+}]_{ext}$	6.1 ± 1.6	632.4 ± 54.3	−43.6 ± 7.1*	7.0 ± 0.6	17
	1 mM $[Ca^{2+}]_{ext}$	5.2 ± 4.1	486.0 ± 59.4	−26.8 ± 13.1	7.2 ± 0.5	3
	1 μM THIP	9.5 ± 14.4	612.5 ± 125	−29.9 ± 17.0	6.7 ± 2.8	4
Interneurons	2 mM $[Ca^{2+}]_{ext}$	5.9 ± 1.6	611.2 ± 36.7	−38.2 ± 5.7*	6.9 ± 0.9	22

Relative to dLGN relay neurons recorded in 2 mM $[Ca^{2+}]_{ext}$, the only significant difference (*$p < 0.05$) between parameters was the reduced frequency of IPSCs recorded in the presence of TTX and the larger peak amplitude of IPSCs in vLGN relay neurons and interneurons.

imposed ion concentrations inherent in this recording configuration. This is also true of gramicidin perforant patch techniques in which sodium and potassium ion concentrations will still be determined by the recording electrode. Therefore, we chose to adopt a cell-attached recording configuration that would have little or no impact on internal ion homeostasis (Fig. 6*A*). As shown in Figure 6*B*, by injecting extracellular current through a relatively "loose seal," we were able to hyperpolarize the recorded neuron sufficiently to generate robust rebound bursts. The properties of these cell-attached bursts (latency to burst generation and the burst frequency) were not significantly different from those we could elicit in the whole-cell configuration (Fig. 6*C*). Under control conditions, dLGN neurons were found to fire a short burst (5 ± 1 spikes; $n = 8$) of high-frequency (307 ± 63 Hz) action potentials after a short delay (33.1 ± 4.1 ms) after the termination of a hyperpolarizing current pulse. Neurons within the vLGN also generated a rebound burst in response to hyperpolarization, although this burst was superimposed on the tonic firing activity of the cell (Fig. 7*B*). The properties of these rebound bursts were comparable with those produced by dLGN neurons, being generated with a similar latency (46.6 ± 11.7 ms; $n = 12$) but exhibiting a significantly slower frequency of firing within the burst (48 ± 11 Hz). For some cells, it was difficult to distinguish the rebound burst from the spontaneous firing activity. Therefore, to separate the effect of the tonic conductance on the burst firing, we only considered action potentials occurring within 400 ms of the termination of the hyperpolarizing step to be part of the burst. This time limit was defined after a visual inspection of our data, which indicated that most cells fired a burst within this interval.

The temporal precision of dLGN burst firing is altered by increasing the tonic $GABA_A$R-mediated conductance

Using recombinant receptors, the GABA agonist THIP has been shown to be a superagonist at δ-$GABA_A$Rs but only a partial agonist at receptors that contain the γ2 subunit (Brown et al., 2002). This pharmacological selectivity has allowed the use of low concentrations of THIP to enhance the tonic conductance mediated by δ-$GABA_A$Rs without having any effect on synaptic $GABA_A$Rs (Belelli et al., 2005; Cope et al., 2005; Jia et al., 2005; Maguire et al., 2005). Therefore, as would be expected, 1 μM THIP enables us to selectively increase the magnitude of the δ-$GABA_A$R-mediated tonic conductance in dLGN relay neurons without altering IPSC properties (see Table 1). On average, all dLGN relay neurons responded to 1 μM THIP with a conductance relative to control of 48.2 ± 26.0 pS/pF ($n = 6$), but no significant THIP-activated conductance was measured in vLGN neurons (0.9 ± 2.2 pS/pF; $n = 8$). In the presence of 1 μM THIP, dLGN relay neurons fire a rebound burst similar to that generated under control conditions (Fig. 7*A*), but the timing of these bursts was altered by activation of δ-$GABA_A$Rs. Therefore, the frequency of spikes within the burst was unchanged (329 ± 69 Hz in control compared with 286 ± 60 Hz in THIP; $n = 6$), as was the number of spikes (5 ± 1 in both cases). However, we observed a significantly longer latency before initiation of the burst (32.9 ± 4.7 ms in control compared with 42.6 ± 4.4 ms in THIP; $n = 6$; see Fig. 7*C*,*D*). We also noticed a significant increase in the variability of the burst latency, with a CV of 0.10 ± 0.03 in control versus 0.24 ± 0.11 in THIP (Fig. 7*D*). In contrast, when we recorded from vLGN, we found that application of 1 μM THIP had no effect on either the latency of the burst (38.5 ± 8.8 ms in control vs 39.0 ± 8.2 ms in THIP; $n = 8$) or the burst frequency (57 ± 20 Hz in control vs 57 ± 18 Hz in THIP). There was also no modulation of the tonic firing activity of these cells (for example, see Fig. 7*B*). This lack of an effect within the vLGN is consistent with the absence of δ-$GABA_A$Rs in this nucleus. However, the enhancement of a tonic $GABA_A$R-mediated conductance within dLGN relay neurons has important consequences for the timing of low-threshold bursts.

Discussion

The expression of α4 and δ subunits correlates well with the presence of a tonic $GABA_A$R-mediated conductance in dLGN (Belelli et al., 2005; Cope et al., 2005). For the first time, we have demonstrated that this tonic $GABA_A$ receptor-mediated conductance is present in adult thalamic relay neurons within the mouse dLGN at physiological temperatures. Furthermore, despite a similar frequency of GABA release in dLGN and vLGN relay neurons, we show that a tonic conductance is not present in vLGN relay neurons, consistent with low levels of α4/δ subunit expression and the absence of a THIP-activated conductance in these neurons. Therefore, high-affinity δ-$GABA_A$Rs appear to be necessary for the generation of a tonic conductance in dLGN relay neurons.

A tonic $GABA_A$R-mediated conductance has now been identified in a number of neuronal types (for review, see Farrant and Nusser, 2005). Studies of the tonic conductance in cerebellar granule cells demonstrate that in immature animals, a large component of this conductance is caused by conventional release of GABA (Kaneda et al., 1995; Brickley et al., 1996; Wall and Usowicz, 1997; Carta et al., 2004), but in adult animals, most of this conductance is attributable to GABA from a source other than conventional vesicular release (Wall and Usowicz, 1997; Rossi et al., 2003; Carta et al., 2004). The source of this GABA is still unknown. In the current study, we have demonstrated that re-

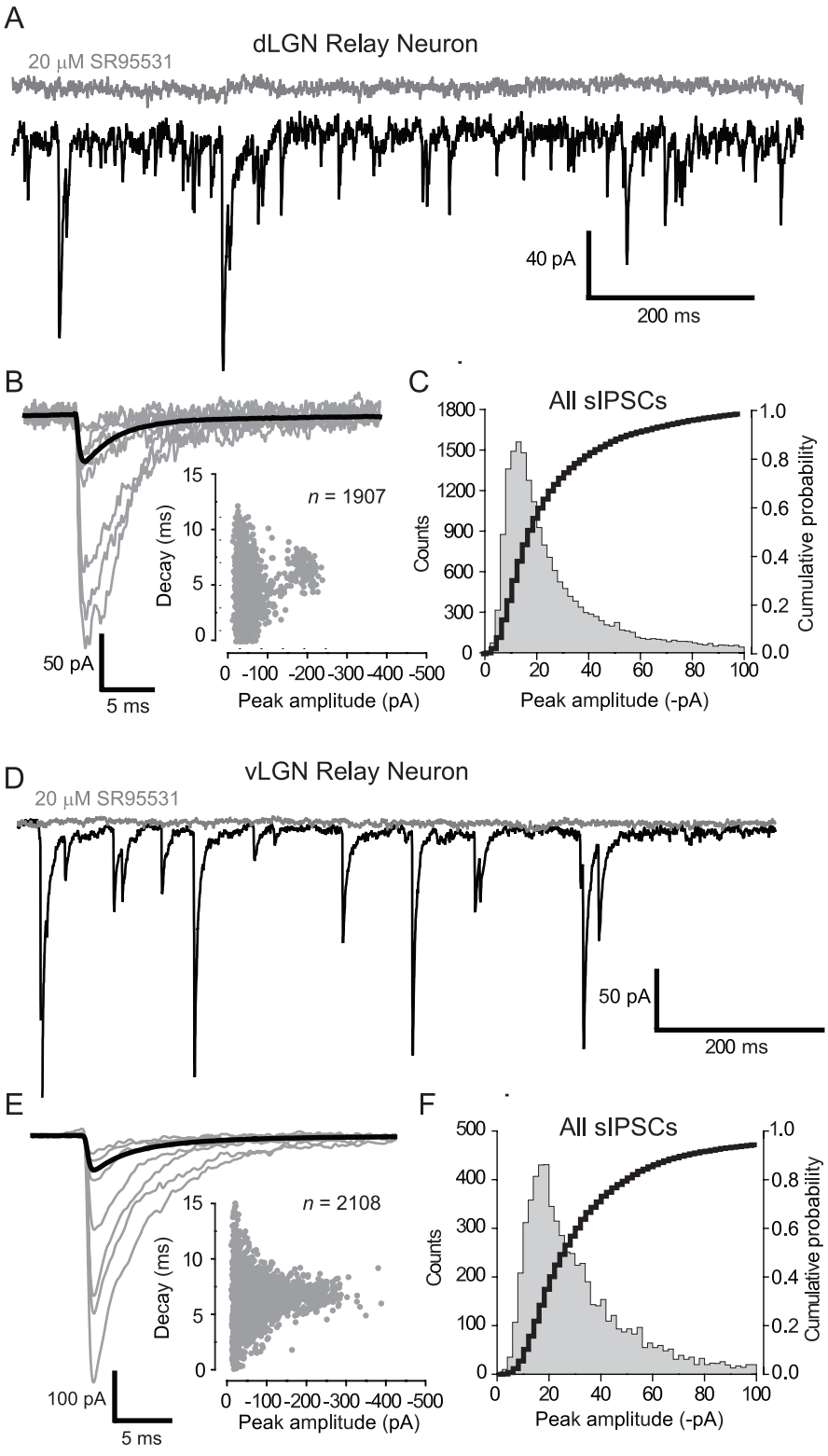

Figure 3. IPSC kinetics are not affected by the presence of δ-$GABA_A$Rs. ***A***, ***D***, Continuous current traces from a dLGN relay neuron (***A***) and a vLGN relay neuron (***D***) before (black trace) and after (gray trace) the application of SR-95531 (20 μM). ***B***, ***E***, Examples of the smallest and largest detected sIPSCs are shown with the average waveform for these cells shown in bold [dLGN neuron (***B***); vLGN neuron (***E***)]. Insets, Plots of peak amplitude against decay time, demonstrating the presence of small and large sIPSCs with similar decay kinetics in each relay neuron. Note how the vLGN relay neuron has a greater proportion of large-amplitude sIPSCs. ***C***, ***F***, All point histogram and cumulative probability plot of sIPSC peak amplitudes recorded from all dLGN ($n = 39$; ***C***) and vLGN ($n = 17$; ***F***) relay neurons. In these graphs, we have restricted the abscissa to a maximum of 100 pA to illustrate the similar distribution of small-amplitude sIPSCs within dLGN and vLGN relay neurons.

ducing the frequency of vesicular GABA release by application of TTX results in a complete loss of the tonic conductance. Therefore, a suitably high ambient GABA concentration would appear to be necessary to generate this tonic conductance in dLGN relay neurons. Indeed, when release probability is low, in 1 mM $[Ca^{2+}]_{ext}$, the frequency of GABA release is also insufficient to generate a tonic $GABA_A$R conductance. It is only in the presence of 2 mM $[Ca^{2+}]_{ext}$ that GABA release is sufficiently high in frequency to generate a tonic conductance. Both of the manipulations of vesicular release that we have made therefore essentially abolish the tonic conductance (87% reduction in TTX and 93% reduction in 1 mM $[Ca^{2+}]_{ext}$), while also causing a decrease in the rate of vesicular release (a decrease in the IPSC frequency of 68% for TTX and of 38% for 1 mM $[Ca^{2+}]_{ext}$). Therefore, the GABA responsible for tonic $GABA_A$R activation appears to come solely from conventional vesicular release, and there is no requirement to invoke any additional source for the GABA in the adult dLGN.

In cerebellar granule cells, activation of high-affinity δ-$GABA_A$Rs is also associated with a prolongation of the postsynaptic conductance (Hamann et al., 2002). However, we see no evidence that δ-$GABA_A$R activation is involved in such a spillover-like phenomenon, given that the spontaneous IPSC decay kinetics were identical in dLGN and vLGN. Also, within the dLGN, when action potential-dependent release is removed, or release probability altered, we do not observe any change in the IPSC kinetics. Moreover, selective activation of δ-$GABA_A$Rs by THIP does not alter the IPSC kinetics in dLGN relay neurons. Therefore, δ-$GABA_A$R activation does not appear to contribute to any component of the phasic IPSC, consistent with a location outside of the synapse for these receptors. Indeed, a recent anatomical study demonstrates that, similar to the situation reported for cerebellar granule cells (Nusser et al., 1998), δ-$GABA_A$Rs in thalamic relay neurons are predominantly extrasynaptic in location (Jia et al., 2005). Although both cerebellar granule neurons and thalamic relay neurons have been shown to express δ subunits, the anatomical location of these receptors, relative to the release sites, could be quite different. For example, the glomerular arrangement in cerebellar granule neurons is such that multiple granule cells project their dendrites into a single glomerulus (Jakab and Hamori, 1988). Therefore, dendritic δ-$GABA_A$Rs could

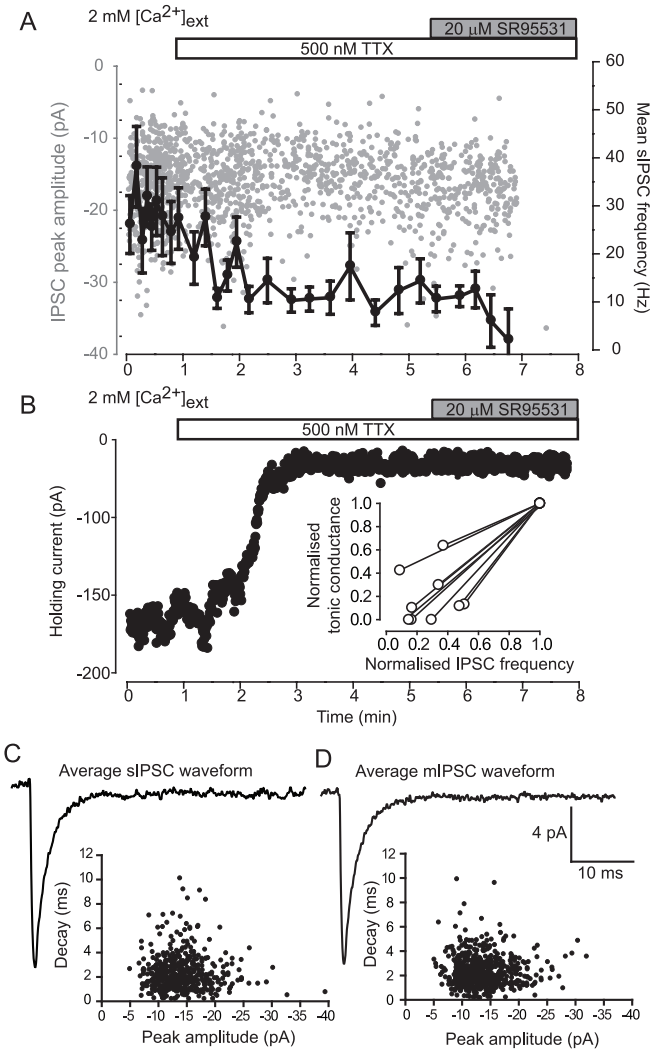

Figure 4. Blockade of action potential-dependent GABA release abolishes the tonic $GABA_A$R-mediated conductance in dLGN relay neurons. ***A***, Plot of individual sIPSC peak amplitude (gray circles) detected during the application of 500 nM TTX (open bar) followed by 20 μM SR-95531 (gray bar). Superimposed onto the same plot is the mean IPSC frequency (solid line) calculated from a running average of 20 consecutive IPSCs. During this experiment, the IPSC frequency gradually reduces in the presence of TTX, and all IPSCs are abolished by the application of SR-95531. ***B***, Plot of the holding current during the same experiment illustrated in ***A***. The holding current is seen to reduce in the presence of TTX, but no further reduction is observed after the application of SR-95531. Inset, The effect of TTX on the tonic $GABA_A$R-mediated conductance and the mean IPSC frequency for all dLGN relay neurons recorded from ($n = 9$). Both of these parameters are normalized to the control values. ***C***, Average IPSC waveform constructed from events detected in the first minute of the control period. A plot of the decay against peak amplitude for all detected sIPSCs is shown in the inset. ***D***, Average IPSC waveform constructed from events recorded in the presence of 500 nM TTX (for events recorded from 5 to 6 min). The plot of decay against peak amplitude for these events shows little change from control. The calibration bar also applies to ***C***.

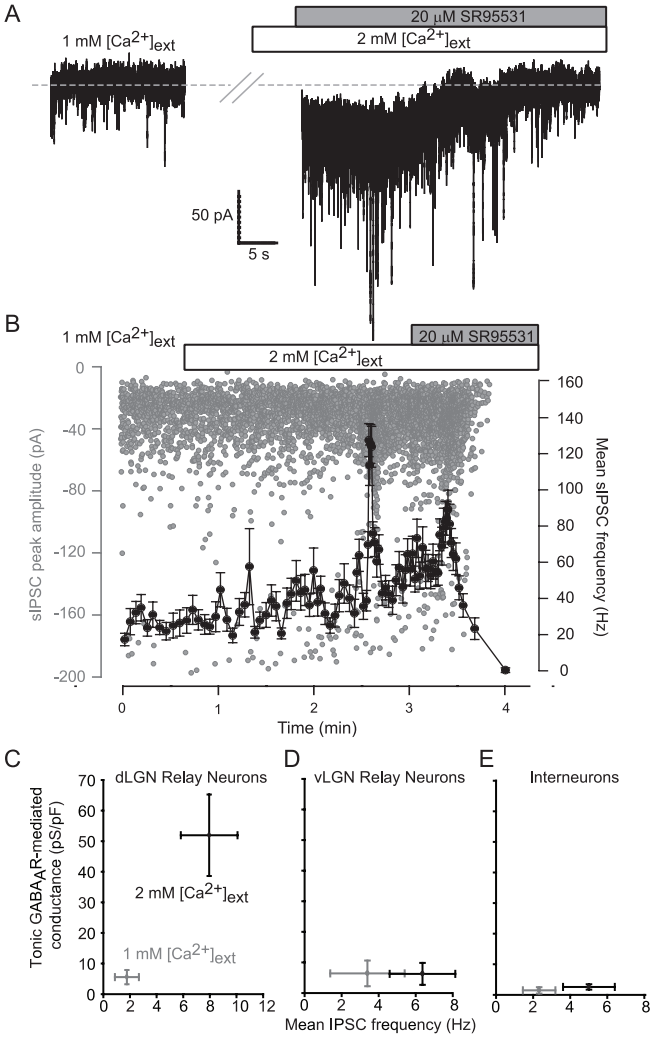

Figure 5. Reducing the frequency of vesicular-dependent GABA release abolishes the tonic $GABA_A$R-mediated conductance in dLGN relay neurons. ***A***, Continuous current record in 1 and 2 mM external Ca^{2+}. Note the increase in both the magnitude of the holding current and the frequency of sIPSCs after switching into 2 mM Ca^{2+}. Application of 20 μM SR-95531 resulted in a reduction in the holding current back to the same magnitude as that observed in 1 mM Ca^{2+} (indicated by gray dashed line). ***B***, Plot of individual sIPSC peak amplitude (gray circles) during the experiment illustrated in ***A***. Superimposed onto this plot is the mean sIPSC frequency (solid line) calculated from a running average of 20 consecutive sIPSCs. ***C–E***, Plots of mean tonic $GABA_A$R-mediated conductance against mean sIPSC frequency for dLGN relay neurons (***C***), vLGN relay neurons (***D***), and interneurons recorded in both dLGN and vLGN (***E***).

be situated only micrometers away from release sites. This situation is ideally suited to spillover. This cannot be assumed to be the case for thalamic glomerular synapses, and extrasynaptic δ-$GABA_A$Rs could simply be located too far from the synapse to be activated fast enough to contribute to the IPSC. However, extrasynaptic δ-$GABA_A$Rs in dLGN relay neurons are capable of sensing global levels of GABA release, because we have demonstrated that the tonic conductance is modulated by manipulations that alter vesicular release. Therefore, in contrast to the situation reported for adult cerebellar granule cells, the tonic conductance in dLGN relay neurons is tightly coupled to synaptic GABA release, providing a dynamic form of inhibition that will reflect the activity within the neuronal network.

In the final set of experiments, we examined the impact of this vesicular-dependent tonic conductance on thalamic relay neuron burst firing using a noninvasive cell-attached recording configuration. We demonstrated a clear increase in the latency and temporal jitter of low-threshold bursts when extrasynaptic δ-$GABA_A$Rs were activated. Burst firing of thalamic relay neurons is a key component in the synchronized oscillatory activity, which occurs in thalamocortical loops during various non-REM sleep states, and also during absence seizures (McCormick and Bal, 1997; Steriade, 1999; Destexhe and Sejnowski, 2003; Llinas

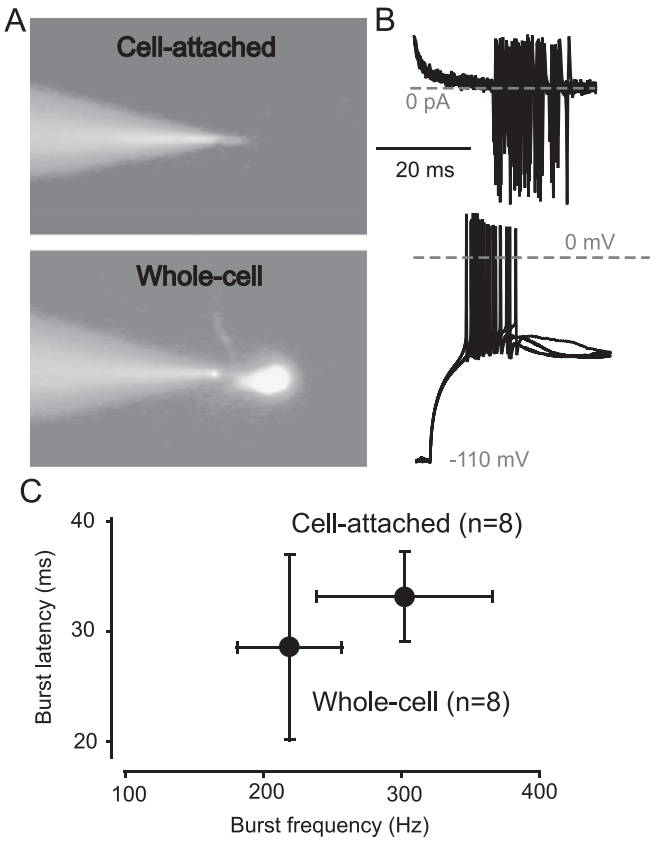

Figure 6. Use of a cell-attached method to elicit low-threshold burst firing. ***A***, Images from the fixed-stage microscope during dLGN relay neuron recording taken during epifluorescence in cell-attached and whole-cell configuration. ***B***, The top trace illustrates cell-attached bursts resulting from extracellular current injection. The bottom trace shows low-threshold bursts recorded in the more conventional whole-cell configuration. In each case, five consecutive records are superimposed to show the variability in burst behavior. ***C***, Quantification of the mean burst frequency and burst latency recorded in cell-attached and whole-cell configuration.

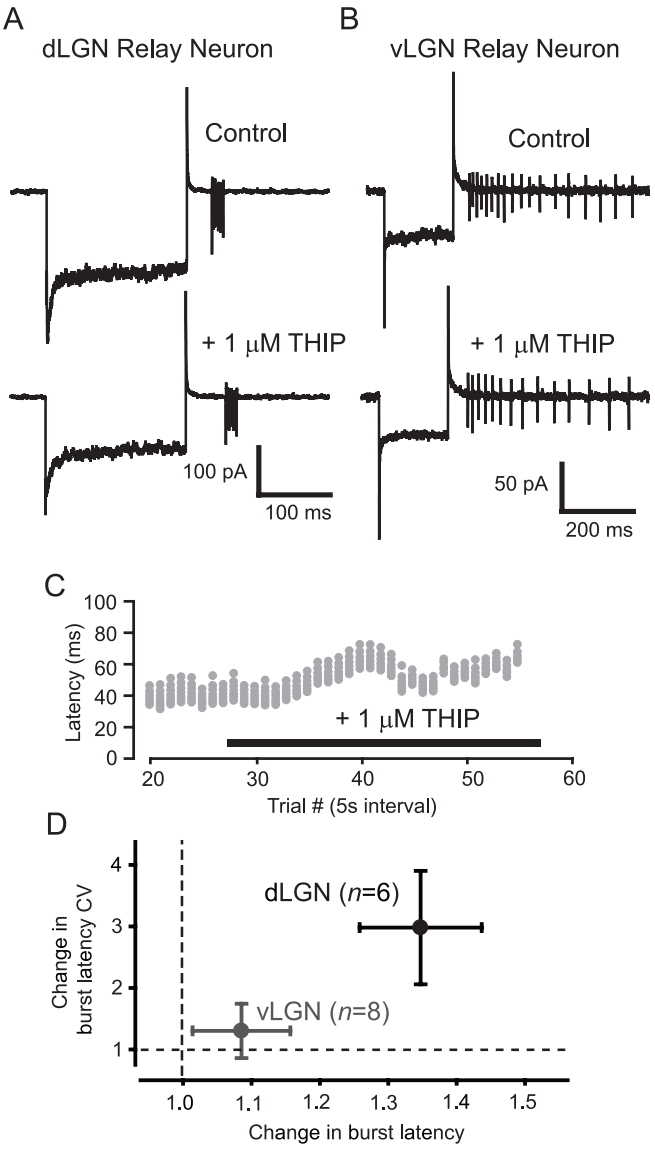

Figure 7. The δ-$GABA_A$R-mediated conductance modulates burst firing in dLGN thalamic relay neurons. ***A***, ***B***, Cell-attached recordings from a dLGN (***A***) and vLGN (***B***) relay neuron before and after THIP application. ***C***, Raster plot of the spikes elicited in response to extracellular current injection during the recording shown in ***A***. In the presence of 1 μM THIP, a clear increase in the latency to first spike is seen, along with an increase in the variability of this delay. However, the number of spikes and the average frequency of these bursts do not alter. ***D***, Quantification of the change in burst latency and the change in the variability (CV) of the burst latency in dLGN and vLGN relay neurons.

and Steriade, 2006). Shunting inhibition offers a simple explanation for the longer latency and increased variability in burst timing that we observe after THIP application in the dLGN. A THIP-induced hyperpolarization of relay neurons has been shown to be permissive for burst firing by removing low-threshold T-type Ca^{2+} channels from inactivation (Cope et al., 2005). Activation of this I_T current and the resulting generation of a burst of action potentials will then be possible. The ability to reach threshold for I_T activation will be further enhanced by the presence of a hyperpolarization-activated cation conductance (I_H) in relay neurons. However, shunting inhibition will reduce the voltage change elicited by a given stimulus and therefore could make it less likely that I_T threshold is reached. It is clear from relay neuron recordings and computer simulations that near-threshold depolarizations lead to longer latency and increased jitter in the timing of low-threshold bursts compared with suprathreshold depolarizations (Zhan et al., 1999). Sohal et al. (2006) have also demonstrated that application of a steady-state hyperpolarizing current increases the burst latency and desynchronizes the response to spindle-like trains of IPSCs injected during current clamp. Therefore, we would predict that increased tonic inhibition could lead to a destabilization of network oscillations in the thalamocortical projection resulting from the increased latency and temporal jitter of low-threshold burst activity in thalamic relay neurons.

The impact of a tonic $GABA_A$R-mediated conductance on network oscillations is clearly very cell-type specific. For example, within the hippocampus, shunting inhibition in interneurons may actually improve the robustness of γ-band oscillations (Vida et al., 2006). In cerebellar granule cells, tonic inhibition is found to generate a change in the gain of the input–output relationship when a physiologically relevant excitation is provided, in the form of a random train of synaptic conductance waveforms (Mitchell and Silver, 2003). Modeling of the cerebellar granule cell layer further suggests that the tonic inhibition in granule cells desynchronizes the oscillatory behavior generated by the Golgi cell–granule cell network during random mossy fiber input (Maex and Schutter, 1998). At concentrations that are selective for activation of δ-$GABA_A$Rs, THIP is a potent hypnotic that

reduces sleep latency and increases sleep duration (Lancel and Faulhaber, 1996; Faulhaber et al., 1997). In humans and rats, THIP appears to promote non-REM sleep, causing increased activity in the δ-band (1–4 Hz) of the EEG (Lancel and Faulhaber, 1996; Faulhaber et al., 1997). However, our data are more consistent with desynchronization of δ-band thalamic oscillations by THIP. When interpreting the effects of drugs like THIP, it is important to remember that expression of δ-$GABA_A$Rs (Pirker et al., 2000; Peng et al., 2002) is not limited to the thalamus, with important δ-$GABA_A$R populations present in the cerebellum (Brickley et al., 2001), hippocampus (Nusser and Mody, 2002), and cortex (Drasbek and Jensen, 2005). Indeed, to fully understand the functional significance of δ-$GABA_A$R expression in regulating specific behavioral states, it will be necessary to consider the differential impact of this type of conductance in a variety of brain regions.

The present study demonstrates that the magnitude of the tonic conductance in adult thalamic relay neurons is correlated with the global level of vesicular GABA release. This particular form of tonic inhibition is therefore sensitive to levels of network activity within the dLGN. Not only would the membrane hyperpolarization that results from this conductance favor thalamic burst firing (Cope et al., 2005), but modulation of the magnitude of this conductance could also alter the timing and variability of these bursts and therefore alter the characteristics of thalamocortical oscillations.

References

Belelli D, Peden DR, Rosahl TW, Wafford KA, Lambert JJ (2005) Extrasynaptic $GABA_A$ receptors of thalamocortical neurons: a molecular target for hypnotics. J Neurosci 25:11513–11520.

Brickley SG, Cull-Candy SG, Farrant M (1996) Development of a tonic form of synaptic inhibition in rat cerebellar granule cells resulting from persistent activation of GABAA receptors. J Physiol (Lond) 497:753–759.

Brickley SG, Revilla V, Cull-Candy SG, Wisden W, Farrant M (2001) Adaptive regulation of neuronal excitability by a voltage-independent potassium conductance. Nature 409:88–92.

Brown N, Kerby J, Bonnert TP, Whiting PJ, Wafford KA (2002) Pharmacological characterization of a novel cell line expressing human alpha(4)beta(3)delta $GABA_A$ receptors. Br J Pharmacol 136:965–974.

Carta M, Mameli M, Valenzuela CF (2004) Alcohol enhances GABAergic transmission to cerebellar granule cells via an increase in Golgi cell excitability. J Neurosci 24:3746–3751.

Cope DW, Hughes SW, Crunelli V (2005) $GABA_A$ receptor-mediated tonic inhibition in thalamic neurons. J Neurosci 25:11553–11563.

De Schutter E (2002) Cerebellar cortex: computation by extrasynaptic inhibition? Curr Biol 12:R363–R365.

Destexhe A, Sejnowski TJ (2003) Interactions between membrane conductances underlying thalamocortical slow-wave oscillations. Physiol Rev 83:1401–1453.

Drasbek KR, Jensen K (2005) THIP, a hypnotic and antinociceptive drug, enhances an extrasynaptic GABAA receptor-mediated conductance in mouse neocortex. Cereb Cortex 16:1134–1141.

Farrant M, Nusser Z (2005) Variations on an inhibitory theme: phasic and tonic activation of GABA(A) receptors. Nat Rev Neurosci 6:215–229.

Faulhaber J, Steiger A, Lancel M (1997) The GABAA agonist THIP produces slow wave sleep and reduces spindling activity in NREM sleep in humans. Psychopharmacology (Berl) 130:285–291.

Hamann M, Rossi DJ, Attwell D (2002) Tonic and spillover inhibition of granule cells control information flow through cerebellar cortex. Neuron 33:625–633.

Jakab RL, Hamori J (1988) Quantitative morphology and synaptology of cerebellar glomeruli in the rat. Anat Embryol 179:81–88.

Jia F, Pignataro L, Schofield CM, Yue M, Harrison NL, Goldstein PA (2005) An extrasynaptic GABAA receptor mediates tonic inhibition in thalamic VB neurons. J Neurophysiol 94:4491–4501.

Kaneda M, Farrant M, Cull-Candy SG (1995) Whole-cell and single-channel currents activated by GABA and glycine in granule cells of the rat cerebellum. J Physiol (Lond) 485:419–435.

Kralic JE, Sidler C, Parpan F, Homanics GE, Morrow AL, Fritschy JM (2006) Compensatory alteration of inhibitory synaptic circuits in cerebellum and thalamus of gamma-aminobutyric acid type A receptor alpha1 subunit knockout mice. J Comp Neurol 495:408–421.

Lam YW, Cox CL, Varela C, Sherman SM (2005) Morphological correlates of triadic circuitry in the lateral geniculate nucleus of cats and rats. J Neurophysiol 93:748–757.

Lancel M, Faulhaber J (1996) The GABAA agonist THIP (gaboxadol) increases non-REM sleep and enhances delta activity in the rat. NeuroReport 7:2241–2245.

Leresche N, Lightowler S, Soltesz I, Jassik-Gerschenfeld D, Crunelli V (1991) Low-frequency oscillatory activities intrinsic to rat and cat thalamocortical cells. J Physiol (Lond) 441:155–174.

Llinas RR, Steriade M (2006) Bursting of thalamic neurons and states of vigilance. J Neurophysiol 95:3297–3308.

Maex R, Schutter ED (1998) Synchronization of golgi and granule cell firing in a detailed network model of the cerebellar granule cell layer. J Neurophysiol 80:2521–2537.

Maguire JL, Stell BM, Rafizadeh M, Mody I (2005) Ovarian cycle-linked changes in GABA(A) receptors mediating tonic inhibition alter seizure susceptibility and anxiety. Nat Neurosci 8:797–804.

McCormick DA, Bal T (1997) Sleep and arousal: thalamocortical mechanisms. Annu Rev Neurosci 20:185–215.

Mitchell SJ, Silver RA (2003) Shunting inhibition modulates neuronal gain during synaptic excitation. Neuron 38:433–445.

Nusser Z, Mody I (2002) Selective modulation of tonic and phasic inhibitions in dentate gyrus granule cells. J Neurophysiol 87:2624–2628.

Nusser Z, Sieghart W, Somogyi P (1998) Segregation of different GABAA receptors to synaptic and extrasynaptic membranes of cerebellar granule cells. J Neurosci 18:1693–1703.

Okada M, Onodera K, Van Renterghem C, Sieghart W, Takahashi T (2000) Functional correlation of GABA(A) receptor α subunits expression with the properties of IPSCs in the developing thalamus. J Neurosci 20:2202–2208.

Pape HC, Budde T, Mager R, Kisvarday ZF (1994) Prevention of Ca(2+)-mediated action potentials in GABAergic local circuit neurones of rat thalamus by a transient K+ current. J Physiol (Lond) 478:403–422.

Peng Z, Hauer B, Mihalek RM, Homanics GE, Sieghart W, Olsen RW, Houser CR (2002) GABA(A) receptor changes in delta subunit-deficient mice: altered expression of alpha4 and gamma2 subunits in the forebrain. J Comp Neurol 446:179–197.

Pirker S, Schwarzer C, Wieselthaler A, Sieghart W, Sperk G (2000) GABA(A) receptors: immunocytochemical distribution of 13 subunits in the adult rat brain. Neuroscience 101:815–850.

Porcello DM, Huntsman MM, Mihalek RM, Homanics GE, Huguenard JR (2003) Intact synaptic GABAergic inhibition and altered neurosteroid modulation of thalamic relay neurons in mice lacking delta subunit. J Neurophysiol 89:1378–1386.

Rossi DJ, Hamann M (1998) Spillover-mediated transmission at inhibitory synapses promoted by high affinity alpha6 subunit GABA(A) receptors and glomerular geometry. Neuron 20:783–795.

Rossi DJ, Hamann M, Attwell D (2003) Multiple modes of GABAergic inhibition of rat cerebellar granule cells. J Physiol (Lond) 548:97–110.

Sassoe-Pognetto M, Panzanelli P, Sieghart W, Fritschy JM (2000) Colocalization of multiple GABA(A) receptor subtypes with gephyrin at postsynaptic sites. J Comp Neurol 420:481–498.

Saxena NC, Macdonald RL (1996) Properties of putative cerebellar gamma-aminobutyric acid A receptor isoforms. Mol Pharmacol 49:567–579.

Sherman SM, Guillery RW (1996) Functional organization of thalamocortical relays. J Neurophysiol 76:1367–1395.

Sohal VS, Pangratz-Fuehrer S, Rudolph U, Huguenard JR (2006) Intrinsic and synaptic dynamics interact to generate emergent patterns of rhythmic bursting in thalamocortical neurons. J Neurosci 26:4247–4255.

Soltesz I, Roberts JD, Takagi H, Richards JG, Mohler H, Somogyi P (1990) Synaptic and nonsynaptic localization of benzodiazepine/GABAA receptor/Cl- channel complex using monoclonal antibodies in the dorsal lateral geniculate nucleus of the cat. Eur J Neurosci 2:414–429.

Stell BM, Brickley SG, Tang CY, Farrant M, Mody I (2003) Neuroactive steroids reduce neuronal excitability by selectively enhancing tonic inhibition mediated by delta subunit-containing GABAA receptors. Proc Natl Acad Sci USA 100:14439–14444.

Steriade M (1999) Coherent oscillations and short-term plasticity in corticothalamic networks. Trends Neurosci 22:337–345.

Sur C, Farrar SJ, Kerby J, Whiting PJ, Atack JR, McKernan RM (1999) Preferential coassembly of alpha4 and delta subunits of the gamma-aminobutyric acidA receptor in rat thalamus. Mol Pharmacol 56:110–115.

Vida I, Bartos M, Jonas P (2006) Shunting inhibition improves robustness of gamma oscillations in hippocampal interneuron networks by homogenizing firing rates. Neuron 49:107–117.

Wall MJ, Usowicz MM (1997) Development of action potential-dependent and independent spontaneous GABAA receptor-mediated currents in granule cells of postnatal rat cerebellum. Eur J Neurosci 9:533–548.

Williams SR, Turner JP, Anderson CM, Crunelli V (1996) Electrophysiological and morphological properties of interneurones in the rat dorsal lateral geniculate nucleus in vitro. J Physiol (Lond) 490:129–147.

Wisden W, Morris BJ (2002) In situ hybridization with oligonucleotide probes. Int Rev Neurobiol 47:3–59.

Zhan XJ, Cox CL, Rinzel J, Sherman SM (1999) Current clamp and modeling studies of low-threshold calcium spikes in cells of the cat's lateral geniculate nucleus. J Neurophysiol 81:2360–2373.

Zhu JJ, Uhlrich DJ (1997) Nicotinic receptor-mediated responses in relay cells and interneurons in the rat lateral geniculate nucleus. Neuroscience 80:191–202.

Zhu JJ, Uhlrich DJ, Lytton WW (1999) Burst firing in identified rat geniculate interneurons. Neuroscience 91:1445–1460.